Development 136, 1859-1868 (2009) doi:10.1242/dev.033498

# Brca1 is required for embryonic development of the mouse cerebral cortex to normal size by preventing apoptosis of early neural progenitors

**Jeremy N. Pulvers and Wieland B. Huttner***

The extent of apoptosis of neural progenitors is known to influence the size of the cerebral cortex. Mouse embryos lacking *Brca1*, the ortholog of the human breast cancer susceptibility gene *BRCA1*, show apoptosis in the neural tube, but the consequences of this for brain development have not been studied. Here we investigated the role of *Brca1* during mouse embryonic cortical development by deleting floxed *Brca1* using *Emx1*-Cre, which leads to conditional gene ablation specifically in the dorsal telencephalon after embryonic day (E) 9.5. The postnatal *Brca1*-ablated cerebral cortex was substantially reduced in size with regard to both cortical thickness and surface area. Remarkably, although the thickness of the cortical layers (except for the upper-most layer) was decreased, cortical layering as such was essentially unperturbed. High levels of apoptosis were found at E11.5 and E13.5, but dropped to near-control levels by E16.5. The apoptosis at the early stage of neurogenesis occurred in both BrdU pulse-labeled neural progenitors and the neurons derived therefrom. No changes were observed in the mitotic index of apical (neuroepithelial, radial glial) progenitors and basal (intermediate) progenitors, indicating that *Brca1* ablation did not affect cell cycle progression. *Brca1* ablation did, however, result in the nuclear translocation of p53 in neural progenitors, suggesting that their apoptosis involved activation of the p53 pathway. Our results show that *Brca1* is required for the cerebral cortex to develop to normal size by preventing the apoptosis of early cortical progenitors and their immediate progeny.

**KEY WORDS: Brca1, Apoptosis, Cerebral cortex**

## INTRODUCTION

The cerebral cortex, which underlies higher brain functions, has undergone a large expansion in size during mammalian evolution, most notably in the primate lineage (Rakic, 1988; Caviness and Takahashi, 1995; Northcutt and Kaas, 1995; Rakic, 1995). Although many intrinsic and extrinsic factors may influence cortical size and cytoarchitecture, such as patterns of neuronal migration (Letinic et al., 2002; Kriegstein and Noctor, 2004; Bystron et al., 2006), thalamic afferents (Windrem and Finlay, 1991; Dehay et al., 2001) and the diversification of subventricular zone neural progenitors (Smart et al., 2002; Haubensak et al., 2004; Miyata et al., 2004; Noctor et al., 2004; Fish et al., 2008), an increase in neuron number during brain development and evolution is ultimately controlled by the number and modes of division of neural progenitors in the embryonic ventricular and subventricular zones (Götz and Huttner, 2005; Kriegstein et al., 2006; Fish et al., 2008).

According to the radial unit hypothesis, the expansion of the neocortex can be explained by increased proliferation of ventricular zone neural progenitors early in development, which dramatically affects the resulting surface area of the neocortex and the number of radially organized columns it contains (Rakic, 1988; Rakic, 1995). On a progenitor cell-intrinsic level, features such as apical-basal polarity, mitotic spindle orientation and cell cycle length are involved in shifting progenitors from proliferation to differentiation, and thus influence cortical size (Bond and Woods, 2006; Buchman and Tsai, 2007; Dehay and Kennedy, 2007; Farkas and Huttner, 2008; Fish et al., 2008).

Max Planck Institute for Molecular Cell Biology and Genetics, Pfotenhauerstrasse 108, 01307 Dresden, Germany.

*Author for correspondence (e-mail: huttner@mpi-cbg.de)

**Accepted 7 April 2009**

Programmed cell death, or apoptosis, is prominent in neural progenitors (Thomaidou et al., 1997) and appears to play an important role in the development of the cerebral cortex as manipulation of this process can greatly alter cortical size (Haydar et al., 1999; Rakic, 2005). Loss of progenitor apoptosis by knockout of caspase 3 (Kuida et al., 1996) or caspase 9 (Kuida et al., 1998) leads to massive overgrowth and folding of the neocortex. Constitutive activation of the Notch signaling pathway in ventricular zone progenitors induces apoptosis, resulting in a reduction in cortical size (Yang et al., 2004). Ephrin A/EphA signaling has also been shown to influence apoptosis and cortical size, whereby gain of EphA receptor function leads to increased apoptosis and a reduction in cortical size, and loss of EphA function leads to a reduction in apoptosis and overgrowth of the neocortex (Depaepe et al., 2005). The cortical surface area reduction seen upon increased Notch and Ephrin A/EphA signaling, and the dramatic cortical surface area increase and convolutions seen in the caspase-deficient mice, are both in accordance with the radial unit hypothesis, which predicts that the loss or increase of early progenitors owing to an increase or decrease, respectively, in apoptosis strongly influences cortical size (Haydar et al., 1999; Rakic, 2005). These observations implicate apoptosis as a developmental, and possibly evolutionary, regulator of cortical size (Haydar et al., 1999).

*BRCA1*, mutations in which predispose women to breast cancer (Miki et al., 1994; Chen et al., 1996; Ruffner and Verma, 1997; Turner et al., 2004), has been implicated in numerous cellular processes, including DNA damage repair (Scully et al., 1997a; Venkitaraman, 2001; Deng and Wang, 2003), cell cycle checkpoints (Wang et al., 2004), transcriptional control (Scully et al., 1997b; Starita et al., 2005), centrosome duplication (Hsu and White, 1998; Xu et al., 1999b; Starita et al., 2004) and mitotic spindle assembly (Joukov et al., 2006). Furthermore, *Brca1* removal causes increased apoptosis in mammary glands (Xu et al., 1999a), epidermis (Berton et al., 2003) and neuroepithelial cells (Gowen et al., 1996; Xu et al.,

2001). *Brca1* is widely expressed in proliferating tissues and is also expressed in the ventricular neuroepithelium of the neural tube (Korhonen et al., 2003).

The relevance of apoptosis in cortical development (Haydar et al., 1999), the increased apoptosis of neuroepithelial cells observed in systemic *Brca1* knockouts (Gowen et al., 1996; Xu et al., 2001), and the expression pattern of *Brca1* in neural progenitors, when considered together, raise the intriguing possibility that *Brca1* might have a role in the development of the cerebral cortex. Moreover, the apparent link between *BRCA1* and the primary microcephaly genes *ASPM* (Bond et al., 2002; Zhong et al., 2005) and *MCPH1* (Xu et al., 2004; Lin et al., 2005), whereby knockdown of either microcephaly gene leads to a decrease in BRCA1 levels, also leads to the question of whether *BRCA1* has a role in brain size regulation. In this context, it is interesting to note that *BRCA1* has undergone positive selection in the primate lineage (Huttley et al., 2000), raising the possibility that it might have been selected owing to a function in brain development. Here, we have investigated this issue by conditional ablation of *Brca1* in cortical progenitors of the dorsal telencephalon during early brain development in the mouse embryo.

## MATERIALS AND METHODS

### Mouse lines and biological samples

Mouse lines were maintained in strict pathogen-free conditions in the animal facility of the Max Planck Institute for Molecular Cell Biology and Genetics, Dresden, Germany. All experiments were performed in accordance with German animal welfare legislation.

A conditional *Brca1* knockout mouse line (Xu et al., 1999a) obtained from the United States National Cancer Institute, Mouse Models of Human Cancers Consortium, Mouse Repository (strain number 01XC8; strain nomenclature: STOCK *Brca1*$^{tm2Cxd}$) was used for this study. The *Emx1*-Cre mouse line was used as a deleter (Iwasato et al., 2000). In all experiments, mice with the genotype *Brca1*$^{loxP/loxP}$ *Emx1-Cre*$^{-/-}$ were used as control, and mice with the genotype *Brca1*$^{loxP/loxP}$ *Emx1-Cre*$^{+/-}$ were used as the conditional knockout. The Z/EG reporter line (Novak et al., 2000) was used to test the specificity of *Emx1*-Cre. Mouse lines and embryos were genotyped for the various alleles by PCR following previously published protocols (Xu et al., 1999a; Iwasato et al., 2000; Novak et al., 2000). The day of the vaginal plug was defined as embryonic day (E) 0.5, and the day of birth was defined as postnatal day (P) 0.5.

### In situ hybridization

In situ hybridization for *Brca1* was performed using a digoxigenin-labeled cRNA antisense probe against exon 11 on 10 μm cryosections by standard methods. Three antisense probes, corresponding to nt 77-948, nt 1008-1912 and nt 2010-2981 of *Brca1* exon 11, were mixed in equal amounts to a final concentration of ~400 ng/ml for the hybridization.

### Histology, immunofluorescence staining and image acquisition

Embryos (E11.5-16.5) and postnatal mice (P4.5, P8.5) were dissected in ice-cold PBS and fixed overnight at 4°C with 4% paraformaldehyde in 120 mM phosphate buffer pH 7.4. For cryosectioning, the samples were further equilibrated at 4°C in 30% sucrose in PBS and then embedded in Tissue-Tek O.C.T. compound (Sakura Finetek) and stored at –20°C. All cryostat sections were cut at 10 μm. For Vibratome sectioning, the fixed samples were embedded in 4% agarose in PBS and cut at 70 μm for E13.5 heads and at 50 μm for E16.5 and postnatal brains. Vibratome sections were collected and stored in PBS until further processing.

Nissl staining was performed using cresyl violet acetate (Sigma) in 40 mM sodium acetate buffer on P4.5 brain Vibratome sections attached to Superfrost Plus microscope slides (Thermo Scientific). Immunofluorescence staining was performed by permeabilizing with 0.3% Triton X-100 in PBS for 30 minutes, quenching with 10 mM $NH_4Cl$ in PBS for 30 minutes, followed by blocking, primary and secondary antibody incubations, and washing in a solution of 0.2% gelatin, 300 mM NaCl and 0.3% Triton X-100 in PBS. For Vibratome sections, the primary antibody was incubated for 2 days at 4°C and the secondary antibody for 2 hours at room temperature. For cryosections, the primary antibody was incubated for 2 hours at room temperature and the secondary antibody for 1 hour at room temperature. All cryosection immunofluorescence staining was performed after antigen retrieval by boiling in a microwave oven in Target Retrieval Solution Citrate pH6 (Dako). All immunofluorescence stainings were co-stained with DAPI (Sigma).

The following primary antibodies were used: Brn1 (sc-6028, Santa Cruz), FoxP2 (ab16046, Abcam), Brn2 (sc-6029, Santa Cruz), Tbr1 (AB9616, Millipore), calretinin (7699/4, Swant), Tuj1 (unconjugated MMS-435P, Alexa Fluor 488-conjugated A488-435L, Covance), active caspase 3 (C8487, Sigma), Pax6 (PRB-278P, Covance), nestin (ab6142, Abcam), BrdU (ab6326, Abcam), phosphohistone H3 (06-570, Millipore), Tbr2 (ab23345, Abcam), p53 (sc-6243, Santa Cruz) and PCNA (PC10, Dako).

Terminal deoxynucleotidyl transferase dUTP nick-end labeling (TUNEL) was performed on cryosections after antigen retrieval and immunofluorescence staining, using the In Situ Cell Death Detection Kit, TMR red (Roche). EGFP in *Emx1-Cre*$^{+/-}$ Z/EG E16.5 brains was detected by intrinsic fluorescence in 50 μm Vibratome sections incubated overnight at 4°C with DAPI in 0.3% Triton X-100 in PBS.

All fluorescence images were acquired by confocal microscopy (Zeiss Axiovert 200M LSM 510). Bright-field images of Nissl staining and in situ hybridization were acquired with an Olympus BX61 microscope fitted with a CCD camera.

### BrdU labeling

BrdU labeling was carried out by intraperitoneal injection of 1.2 mg BrdU (Sigma) in 120 μl PBS into pregnant females 11.5 days post-coitum. Mice were sacrificed 1, 2, 4 or 6 hours after injection, and embryos were processed for cryosectioning as described above. For BrdU immunofluorescence in combination with TUNEL staining, cryosections were subjected to antigen retrieval as described above, then permeabilized with 0.3% Triton X-100 in PBS for 30 minutes, quenched with 10 mM $NH_4Cl$ in PBS for 30 minutes, and then the TUNEL reaction was performed. Cryosections were then subjected to a 30-minute 2 M HCl treatment at 37°C, followed by blocking, primary and secondary antibody incubations, and washing in 10% horse serum in PBS.

### Quantifications

Quantification of DAPI, TUNEL, BrdU, phosphohistone H3 and Tbr2 stainings was performed on 200-μm-wide fields with the ventricular surface horizontal. Quantification of Brn1, FoxP2, Brn2 and Tbr1 stainings was performed on 300-μm-wide fields with the pial surface horizontal. Brn1/FoxP2 double-immunofluorescence images were used to define single-positive ($Brn1^+$ or $FoxP2^+$) and double-positive ($Brn1^+$ $FoxP2^+$) cells and to determine their distribution across the cortical wall. The ventricular surface length was measured by tracing the apical surface from the most dorsal point down to the attachment site of the ganglionic eminence using ImageJ (NIH). For each anatomical location, the mean was taken from the left and right ventricle, and then the mean was taken from a total of three embryos each for the control and conditional knockout. For all quantifications, the embryos and brains were taken from at least two litters, except for those shown in Fig. 3, which were from one litter. All embryonic cell counting was performed on images from the dorsal telencephalon in regions represented by the white box in Fig. 3A′. *P*-values were calculated by Student's *t*-test.

## RESULTS

### Conditional ablation of *Brca1* in neural progenitors of the mouse embryonic dorsal telencephalon results in a smaller neocortex

To study the role of Brca1 in the development of the cerebral cortex, *Brca1* was selectively ablated in the mouse embryonic dorsal telencephalon (the future neocortex, hippocampus and olfactory bulb) by crossing a mouse line carrying a *Brca1* allele in which exon 11 is flanked by loxP sites (Xu et al., 1999a) with an *Emx1*-Cre knock-in line (Iwasato et al., 2000). In the resulting *Brca1*

conditional exon 11-deleted mice, the Brca1 protein lacks ~60% of its sequence, including various domains crucial for its function (Xu et al., 1999a). Recombination by *Emx1*-Cre in the dorsal telencephalon is known to start at E9.5 (Iwasato et al., 2000) and hence occurs in neuroepithelial cells, the primary neural progenitors of the neocortex. This enabled us to specifically study the function of Brca1 in these progenitors and their progeny during cortical development.

In the experiments described below, mice homozygous for the floxed *Brca1* allele but lacking an *Emx1*-Cre allele (*Brca1*$^{loxP/loxP}$ *Emx1-Cre*$^{-/-}$) were used as the control, and mice homozygous for the floxed *Brca1* allele but carrying an *Emx1*-Cre allele (*Brca1*$^{loxP/loxP}$ *Emx1-Cre*$^{+/-}$) were used as the conditional knockout (cKO).

In situ hybridization for *Brca1* mRNA on E11.5 cryosections using an antisense probe against exon 11 showed that in the E11.5 control telencephalon, *Brca1* is expressed in the ventricular zone (VZ) but not in the neuronal layers (Fig. 1A, left), as previously reported (Korhonen et al., 2003). *Brca1* mRNA was predominantly located in the basal (abventricular) half of the VZ, which is likely to reflect the specific expression of *Brca1* in late G1, S and G2 phase (Gudas et al., 1996; Vaughn et al., 1996). Upon conditional ablation by *Emx1*-Cre, *Brca1* mRNA was not detected in the E11.5 dorsal telencephalon but was still expressed in the ganglionic eminences of the ventral telencephalon (Fig. 1A, right). This demonstrated the regional specificity of *Brca1* ablation, consistent with specific expression of *Emx1*-Cre in the dorsal telencephalon (Iwasato et al., 2000), which we confirmed for E16.5 embryos by crossing to the Z/EG reporter line (Novak et al., 2000), in which EGFP is overexpressed upon loxP recombination (Fig. 1B).

To examine the effects of conditional *Brca1* ablation on the neocortex, we first analyzed the size and gross morphology of the P4.5 brain. Compared with the control, *Brca1*-ablated brains showed a reduction in size specific to the cerebral cortex (Fig. 1C). The whole-brain weight of *Brca1*-ablated mice was also significantly reduced (Fig. 1D). Analysis of anatomically matched, Nissl-stained coronal sections of P4.5 brains revealed that the reduction in size upon *Brca1* ablation affected the neocortex and hippocampus (Fig. 1E-F′). Importantly, the decrease in neocortex size concerned both the lateral (Fig. 1E,F, dotted lines) and radial (Fig. 1E,F, solid lines) dimension. Remarkably, conditionally *Brca1*-ablated mice developed to adulthood without obvious effects on health and fertility. A reduced cerebral cortex was not observed in *Brca1* heterozygous, *Emx1*-Cre-positive (*Brca1*$^{loxP/wt}$ *Emx1-Cre*$^{+/-}$) P4.5 mice (data not shown), indicating that the conditional removal of one *Brca1* allele, or the expression of Cre recombinase as such, had no effect on cerebral cortex size.

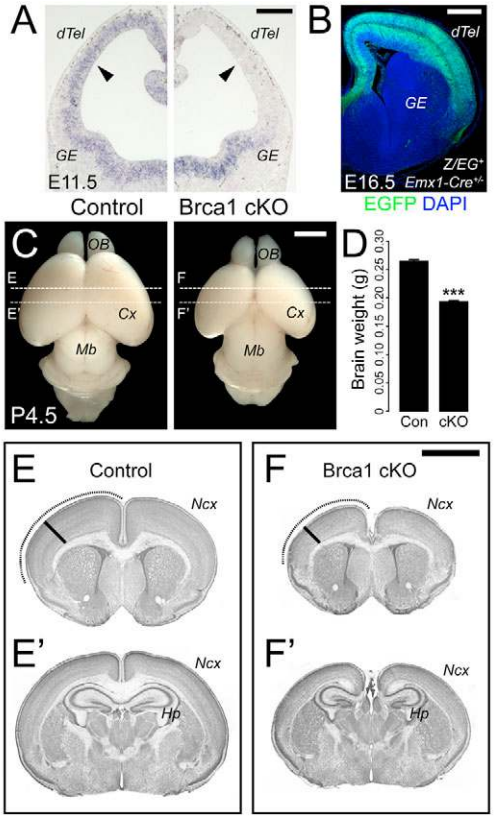


**Fig. 1. Conditional ablation of *Brca1* in neural progenitors of the mouse embryonic dorsal telencephalon results in a smaller neocortex.** (**A**) *Brca1* exon 11 in situ hybridization on coronal 10-μm cryosections of E11.5 telencephalon of control (*Brca1*$^{loxP/loxP}$ *Emx1-Cre*$^{-/-}$, left) and *Brca1* conditional knockout (cKO; *Brca1*$^{loxP/loxP}$ *Emx1-Cre*$^{+/-}$, right) mice. Note the lack of *Brca1* expression in the dorsal telencephalon (*dTel*, arrowheads) upon conditional ablation of *Brca1*. *GE*, ganglionic eminence. (**B**) Merged image (6-μm optical section) showing EGFP intrinsic fluorescence (green) and DAPI staining (blue) of a coronal Vibratome section of E16.5 telencephalon of a *Emx1-Cre*$^{+/-}$ Z/EG mouse. Note the specific expression of EGFP in the dorsal telencephalon. (**C**) P4.5 brains of *Brca1* control and cKO mice. Note the reduction in the size of the cerebral cortex (*Cx*) upon conditional ablation of *Brca1*. *OB*, olfactory bulb; *Mb*, midbrain. Dashed lines indicate the positions of the coronal Nissl-stained sections shown in E-F′. The distance between the more rostral (E,F) and more caudal (E′,F′) sections is 900 μm. (**D**) Brain weight of *Brca1* control (Con) and cKO mice at P4.5; data are the mean of 13 and 10 pups, respectively; error bars indicate s.e.m.; ***$P$<0.001. (**E-F′**) Nissl staining of coronal 50-μm Vibratome sections of P4.5 *Brca1* control (E,E′) and cKO (F,F′) mice. Note the reduction in the size of the neocortex (*Ncx*) in both the radial (solid lines) and lateral (dotted lines) dimensions and the smaller hippocampus (*Hp*) upon conditional ablation of *Brca1*. Scale bars: 250 μm in A; 500 μm in B; 2 mm in C,E-F′.

## Conditional ablation of *Brca1* results in a reduced number of deep-layer, but not of upper-most layer, neurons

To investigate the nature of the reduction in the radial thickness of the *Brca1*-ablated neocortex, we analyzed P4.5 and P8.5 coronal brain sections for the expression of markers of certain cortical layers. We performed double immunofluorescence for FoxP2, which is predominantly expressed by early-born, deep-layer neurons (Ferland et al., 2003), together with Brn1 (Pou3f3 – Mouse Genome Informatics), which is predominantly expressed by later-born, upper-layer neurons (He et al., 1989; McEvilly et al., 2002), and also for Tbr1, which is strongly expressed by layer VI and layer III neurons (Bulfone et al., 1995; Hevner et al., 2001), together with Brn2 (Pou3f2), which is predominantly expressed by later-born, upper-layer neurons (He et al., 1989; McEvilly et al., 2002). This revealed the preservation of cortical layering in the conditional *Brca1* knockout, with Brn1$^+$ and Brn2$^+$ neurons still preferentially found in the upper layers and FoxP2$^+$ and Tbr1$^+$ neurons preferentially in the deeper layers (Fig. 2A,B; see Fig. S1A in the supplementary material).

Cortical organization was further examined by immunofluorescence staining on P4.5 coronal brain sections for calretinin (calbindin 2), which, at early postnatal stages, is expressed

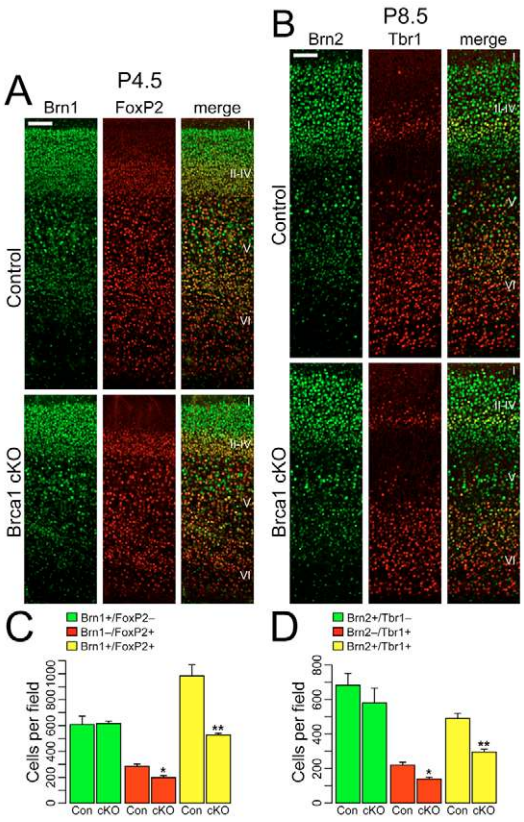


**Fig. 2. Conditional ablation of *Brca1* results in a reduced number of deep-layer, but not of upper-most layer, neurons.** (**A**,**B**) Double immunofluorescence (6-μm optical sections) for the upper-layer marker Brn1 (green) and the deep-layer marker FoxP2 (red) on Vibratome sections of P4.5 neocortex (A), and for the upper-layer marker Brn2 (green) and the deep-layer marker Tbr1 (red) on Vibratome sections of P8.5 neocortex (B) of *Brca1* control (top) and cKO (bottom) mice. Sections in A were consecutive to the Nissl-stained sections shown in Fig. 1E,F, with the fields shown corresponding to the position of the solid lines in Fig. 1E,F. Cortical layers are indicated by I-VI. Scale bars: 100 μm. (**C**,**D**) Quantification of Brn1$^+$ FoxP2$^-$ (green), Brn1$^-$ FoxP2$^+$ (red) and Brn1$^+$ FoxP2$^+$ (yellow) cells (C), and of Brn2$^+$ Tbr1$^-$ (green), Brn2$^-$ Tbr1$^+$ (red) and Brn2$^+$ Tbr1$^+$ (yellow) cells (D), in a 300-μm-wide segment of the cortical wall of *Brca1* control (Con) and cKO mice as shown in A and B, respectively. Data are the mean of three brains (one field per brain); error bars indicate s.e.m.; *$P$<0.05, **$P$<0.01.

by neurons in layer I (specifically Cajal-Retzius cells) (Del Río et al., 1995; Fonseca et al., 1995), pyramidal-like neurons in layer V (Schierle et al., 1997) and interneurons (Rogers, 1992; Wonders and Anderson, 2006). The abundance and organization of calretinin$^+$ neurons appeared unaffected in the *Brca1*-ablated neocortex as compared with the control (see Fig. S2 in the supplementary material).

Given the reduction in the overall thickness of the *Brca1*-ablated neocortex, we next quantified the number of neurons positive for the aforementioned markers to see whether this reduction occurred equally in all cortical layers or in only a particular layer or neuron subpopulation. We defined three neuronal subpopulations, i.e. the Brn1$^+$ (green) and FoxP2$^+$ (red) single-positive and the FoxP2$^+$ Brn1$^+$ double-positive (yellow) neurons, the distribution of which across the cortical wall is illustrated by the colored dots in Fig. S1B in the supplementary material. Interestingly, at P4.5 (Fig. 2C) and P8.5 (see Fig. S1C in the supplementary material), whereas the number of FoxP2$^+$ and of FoxP2$^+$ Brn1$^+$ neurons in a 300-μm-wide segment of the cortical wall was reduced to almost half upon *Brca1* ablation, the number of Brn1$^+$ but FoxP2$^-$ neurons, which were predominantly found in the upper-most layer, was unaffected. Similarly, at P8.5, whereas the number of Tbr1$^+$ and of Tbr1$^+$ Brn2$^+$ neurons in a 300-μm-wide segment of the cortical wall was reduced to almost half upon *Brca1* ablation, the number of Brn2$^+$ but Tbr1$^-$ neurons, which were predominantly found in the upper-most layer, showed only a slight (statistically insignificant) reduction (Fig. 2D). Taken together, these data indicated that the reduction in overall cortical thickness (Fig. 1E-F′; Fig. 2A,B; see Fig. S1A in the supplementary material) was not due to a reduction in late-born neurons, but primarily reflected a decrease in earlier-born neurons.

## The ventricular surface and progenitor number are reduced in the *Brca1*-ablated E13.5 dorsal telencephalon

To elucidate the developmental basis of the reduction in radial thickness of the postnatal neocortex (Fig. 2), and also to investigate the reduction in the lateral expansion of the neocortex (Fig. 1E-F′), we analyzed the effects of *Brca1* ablation during embryonic cortical development. We first quantified the lateral extension of the VZ of the E13.5 dorsal telencephalon, which reflects neural progenitor number. For this purpose, E13.5 brains were subjected to serial Vibratome coronal sectioning followed by DAPI staining, and the length of the ventricular surface was compared between the control and *Brca1*-ablated dorsal telencephalon at three defined, anatomically corresponding regions along the rostrocaudal axis (Fig. 3A-A″). At each of these three regions, the length of the ventricular surface was significantly reduced, by one-third to half, upon *Brca1* ablation (Fig. 3B-B″).

We complemented this analysis of VZ lateral extension by determining the abundance of DAPI-stained nuclei in the radial dimension of the progenitor layers. Using Tuj1 (Tubb3) immunostaining to distinguish the preplate from the subventricular zone (SVZ) and VZ, this revealed a decrease in the radial thickness of the progenitor layers in the E13.5 *Brca1*-ablated dorsal telencephalon (Fig. 3C,C′), which is likely to reflect the significant reduction in progenitor nuclei number found upon quantification (Fig. 3D, gray columns). By contrast, there was no detectable difference in the number of neuronal nuclei in the preplate at this developmental stage (Fig. 3D, green columns). Taken together, the reduction in both lateral ventricular length (Fig. 3A-B″) and progenitor layer radial thickness (Fig. 3C,D) at E13.5 indicates a decrease in the number of neocortical progenitors at this relatively early stage of neurogenesis.

## Conditional *Brca1* ablation in the dorsal telencephalon causes massive apoptosis in progenitor and neuronal layers at E11.5 and E13.5, but not at E16.5

The decrease in neocortical progenitor number upon *Brca1* ablation could be due to reduced proliferation and/or cell death. In fact, DAPI staining did show numerous pyknotic nuclei in the progenitor layers of the *Brca1*-ablated E13.5 dorsal telencephalon (Fig. 3C′, arrowheads). Given also that *Brca1* removal in other systems has been reported to result in increased apoptosis (Gowen et al., 1996; Xu et al., 1999a; Xu et al., 2001; Berton et al., 2003),

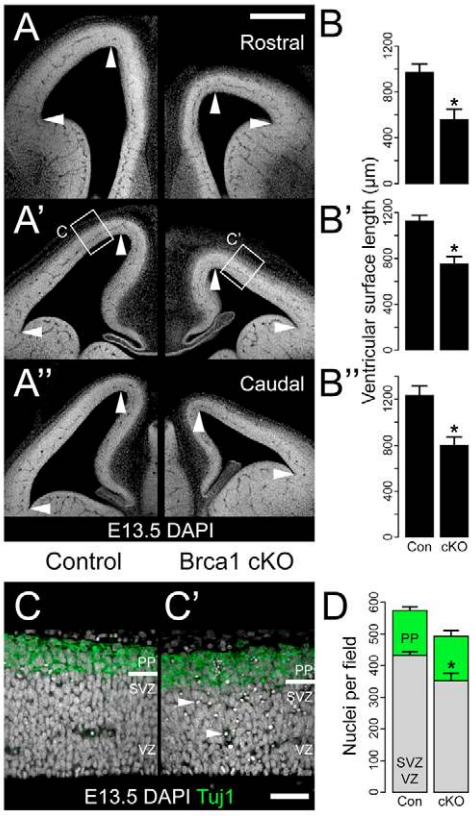


**Fig. 3. Ventricular surface and progenitor number are reduced in the *Brca1*-ablated E13.5 dorsal telencephalon.** (**A-A″**) DAPI staining (6-μm optical sections) of coronal Vibratome sections of E13.5 telencephalon of *Brca1* control (left) and cKO (right) mice. Sections shown are from three different positions along the rostrocaudal axis, as indicated. (**B-B″**) Quantification of ventricular surface length between the positions indicated by arrowheads in the corresponding A-A″. Data are the mean of three embryos (one section per embryo); error bars indicate s.e.m.; **P*<0.05. (**C**,**C′**) Immunofluorescence (1-μm optical section) for the neuronal marker Tuj1 (green) combined with DAPI staining (white) in the region of the dorsal telencephalon indicated by the boxes in A′. Arrowheads indicate pyknotic apoptotic nuclei. PP, preplate. (**D**) Quantification of DAPI-stained nuclei (excluding pyknotic apoptotic nuclei) in the ventricular zone (VZ) plus subventricular zone (SVZ) (gray) and preplate (PP, identified by Tuj1 immunofluorescence, green) in a 200-μm-wide segment of the cortical wall as shown in C,C′. Data are the mean of three embryos (one field per embryo); error bars indicate s.e.m.; **P*<0.05. Scale bars: 400 μm in A-A″; 50 μm in C.

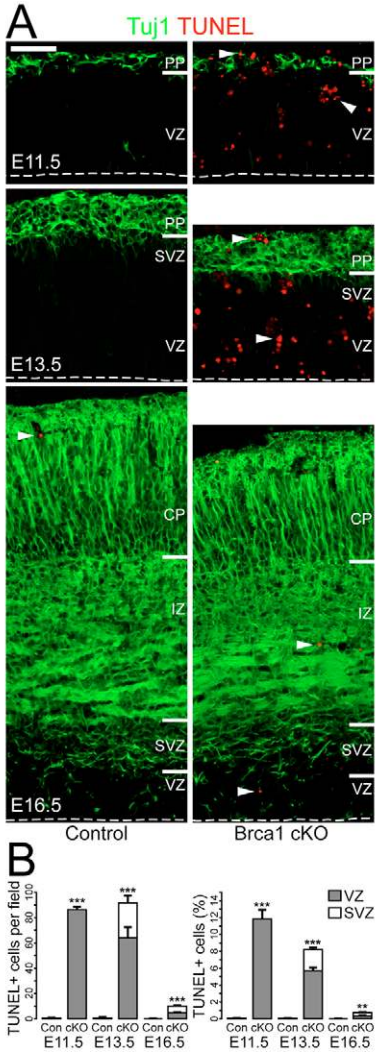


**Fig. 4. Conditional *Brca1* ablation in the dorsal telencephalon causes massive apoptosis in progenitor and neuronal layers at E11.5 and E13.5, but not at E16.5.** (**A**) Immunofluorescence for Tuj1 (green) and TUNEL staining (red) of coronal cryosections (1-μm optical section) of E11.5, E13.5 and E16.5 dorsal telencephalon of *Brca1* control (left) and cKO (right) mice. PP, preplate; IZ, intermediate zone; CP, cortical plate. Dashed lines indicate the ventricular surface. Scale bar: 50 μm. (**B**) Quantification of TUNEL-positive nuclei in the VZ (gray) and SVZ (white) as shown in A, expressed as the number per field (left) or as a percentage of the total progenitor layer (VZ+SVZ) nuclei as revealed by DAPI staining (including pyknotic apoptotic nuclei) (right), in *Brca1* control (Con) and cKO mice. Data are the mean of three embryos (the sum of three 200-μm-wide fields per embryo); error bars indicate s.e.m.; ***P*<0.01, ****P*<0.001.

we analyzed *Brca1* control and cKO embryos at three different stages of cortical neurogenesis (E11.5, E13.5, E16.5) for apoptosis by TUNEL staining. Numerous TUNEL-positive pyknotic nuclei were detected in the *Brca1*-ablated cortical wall at E11.5 and E13.5, being present in both the progenitor layers (VZ plus SVZ) and the preplate, as identified by Tuj1 immunostaining (Fig. 4A). The majority of the cells with TUNEL-positive nuclei also showed immunoreactivity for active caspase 3 (data not shown). By contrast, very few apoptotic nuclei were detected in the E16.5 *Brca1*-ablated cortical wall (Fig. 4A); at this stage, a decrease in the radial thickness of the cortical plate was evident.

Quantification of TUNEL-positive nuclei in the progenitor layers, i.e. the VZ at E11.5 and the VZ and SVZ at E13.5 and E16.5, in the *Brca1*-ablated dorsal telencephalon revealed a dramatically increased absolute number (Fig. 4B, left) and proportion (Fig. 4B, right) at the early stages of neurogenesis (E11.5 and E13.5) as compared with the control. Both the VZ (Fig. 4B, gray column segments) and SVZ (Fig. 4B, white column segments) were found to contain apoptotic cells. There was also a substantial number of apoptotic nuclei in the preplate (51±4 and 45±11 nuclei per field at E11.5 and E13.5, respectively; data not illustrated). By contrast, at E16.5, the absolute number and proportion of apoptotic nuclei in the progenitor layers were much lower, albeit still significantly higher than in the control (Fig. 4B).

### Identification of apoptotic cells in the E11.5 VZ as progenitors by BrdU pulse-chase

Whereas the TUNEL-positive cells in the preplate were most likely to be postmitotic neurons (Fig. 4A), the apoptotic cells in the progenitor layers could be progenitors, newborn neurons, or both. To directly investigate apoptosis of VZ progenitors, we performed immunofluorescence for the VZ progenitor marker Pax6 (Götz et al., 1998) in combination with TUNEL staining. This revealed a small number of TUNEL-positive cells with Pax6 immunoreactivity (see Fig. S3 in the supplementary material), suggesting that VZ progenitors underwent apoptosis upon conditional *Brca1* ablation (although we cannot exclude the possibility that the apoptotic cells also included newborn neurons that had inherited the Pax6 protein). However, most apoptotic nuclei in the VZ, although apparently surrounded by nestin$^{+}$ cytoplasm (see Fig. S3 in the supplementary material), did not show Pax6 immunoreactivity, which most likely reflected proteolysis during the process of apoptosis (Taylor et al., 2008).

To obtain more compelling evidence for the apoptosis of VZ progenitors, we performed BrdU pulse-chase at E11.5 and determined the time course of the appearance of TUNEL-positive BrdU-labeled cells. Embryos were analyzed 1, 2, 4 and 6 hours after a single BrdU administration for BrdU-labeled nuclei and TUNEL staining. BrdU immunofluorescence showed that 1 and 2 hours after BrdU administration, most labeled nuclei were found in the basal half of the VZ (Fig. 5A,B), whereas after 4 and 6 hours, most labeled nuclei were located in its apical half (Fig. 5C,D), documenting the basal-to-apical interkinetic nuclear migration of VZ progenitors during their G2 phase (Götz and Huttner, 2005). The proportion of BrdU-labeled nuclei was essentially the same for control and *Brca1*-ablated dorsal telencephalon (Fig. 5F). Importantly, analysis of the *Brca1*-ablated dorsal telencephalon for BrdU-labeled nuclei in the VZ that became TUNEL-positive (Fig. 5E) showed that these appeared rapidly after BrdU administration, being observed at the earliest time point analyzed (1 hour after BrdU) and increasing thereafter (Fig. 5G). By contrast, a much lower proportion of TUNEL-positive BrdU-labeled nuclei and no increase over time were observed for the control (Fig. 5G). Given the average length of the S and G2 phases of VZ progenitors in the E11.5 dorsal telencephalon of ~3 hours and ~2 hours, respectively (Takahashi et al., 1995; Calegari et al., 2005), these data imply that most of the TUNEL-positive BrdU-labeled cells observed during the BrdU pulse-chase were VZ progenitors in the S or G2 phase (rather than neurons derived therefrom), and hence provide strong evidence for substantial apoptosis of VZ progenitors upon *Brca1* ablation.

### Conditional *Brca1* ablation in the dorsal telencephalon does not alter the mitotic index of apical and basal progenitors

To address whether the reduction in neocortical progenitors in the *Brca1*-ablated dorsal telencephalon was caused by reduced proliferation, we performed immunofluorescence for the M-phase marker phosphohistone H3 in combination with DAPI staining (Fig. 6A), and quantified the mitotic index for apical mitoses and basal mitoses in the VZ (E11.5) or VZ plus SVZ (E16.5) (Fig. 6B). At both E11.5 and E16.5 there was no significant difference in the mitotic index of either class of mitoses between the control and *Brca1*-ablated dorsal telencephalon. However, in line with the reduction in the number of nuclei per field in the progenitor layers that we observed at E11.5 (Fig. 6A,C; see also Fig. 3D and Fig. 7B for E13.5) but no longer at E16.5, the abundance (as opposed to the mitotic index) of apical and basal mitoses at E11.5 was decreased accordingly (data not shown). We conclude that, in line with the observation that in the E11.5 *Brca1*-ablated dorsal telencephalon the labeling index 1 hour after BrdU administration is the same as in the control (Fig. 5F), cell cycle progression was unaffected upon *Brca1* ablation.

### Conditional *Brca1* ablation in the dorsal telencephalon does not alter the proportion of Tbr2-positive cells

To analyze whether the reduction in neocortical progenitor number and radial thickness of the neocortex upon *Brca1* ablation was attributable to a specific lineage change at the progenitor level, we

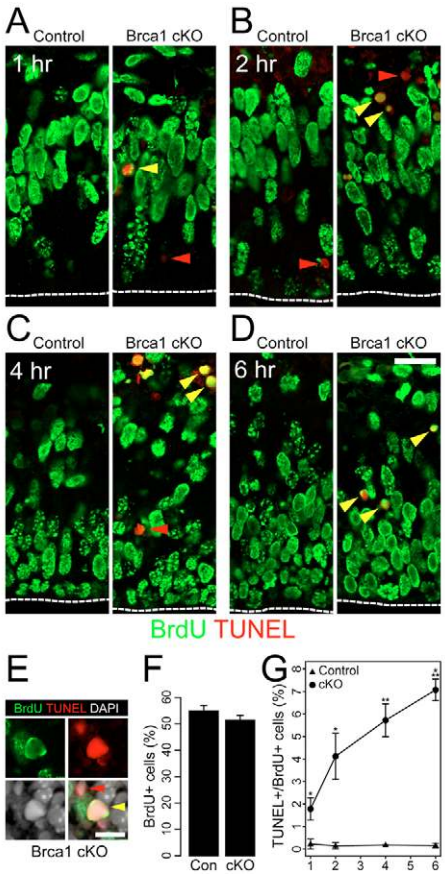


**Fig. 5. BrdU pulse-labeled E11.5 VZ progenitors undergo apoptosis.** (**A-E**) Immunofluorescence for BrdU (green) and TUNEL staining (red) of coronal cryosections (1-μm optical sections) of E11.5 dorsal telencephalon of *Brca1* control (A-D, left) and cKO (A-D, right and E) mice. Embryos were analyzed 1 (A,E), 2 (B), 4 (C) and 6 (D) hours after a single administration of BrdU. Dashed lines indicate the ventricular surface, and the top of the image is the pial surface. Examples of TUNEL-positive BrdU-negative cells are indicated by red arrowheads; examples of TUNEL-positive BrdU-positive cells are indicated by yellow arrowheads. In E, DAPI staining is shown in white. (**F**) Quantification of BrdU-positive nuclei, expressed as a percentage of total nuclei (including pyknotic apoptotic nuclei) as revealed by DAPI staining, in the VZ of E11.5 dorsal telencephalon of *Brca1* control (Con) and cKO mice collected 1 hour after BrdU administration. Data are the mean of three embryos (the sum of three 200-μm-wide fields per embryo) from two BrdU-injected mothers; error bars indicate s.e.m. (**G**) Quantification of TUNEL-positive BrdU-positive nuclei, expressed as a percentage of the total BrdU-positive nuclei, in the E11.5 dorsal telencephalon of *Brca1* control and cKO mice collected 1, 2, 4 and 6 hours after BrdU administration. Data are the mean of three embryos (the sum of three 200-μm-wide fields per embryo) from two BrdU-injected mothers; error bars indicate s.e.m.; **P*<0.05, ***P*<0.01, ****P*<0.001. Scale bars: 20 μm in A-D; 10 μm in E.

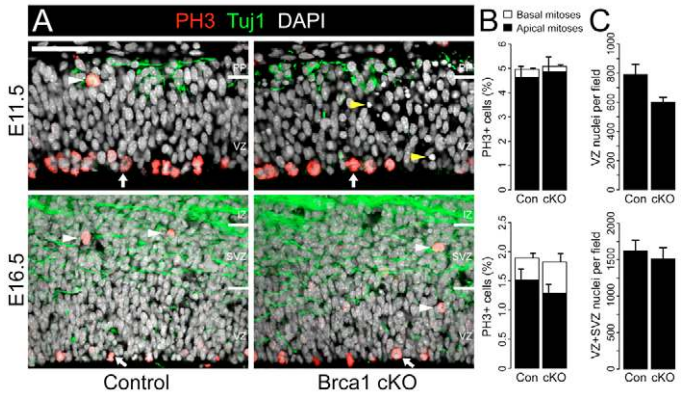


**Fig. 6. Conditional *Brca1* ablation in the dorsal telencephalon does not alter the mitotic index of apical and basal progenitors.** (**A**) Double immunofluorescence (1-μm optical sections) for phosphohistone H3 (PH3, red) and Tuj1 (green) combined with DAPI staining (white) of coronal cryosections of E11.5 (top) and E16.5 (bottom) dorsal telencephalon of *Brca1* control (left) and cKO (right) mice. Examples of phosphohistone H3$^+$ apical and basal mitoses are indicated by arrows and arrowheads, respectively; yellow arrowheads indicate pyknotic apoptotic nuclei. PP, preplate; IZ, intermediate zone. Scale bar: 50 μm. (**B**) Quantification of phosphohistone H3$^+$ apical (black) and basal (white) mitoses, expressed as a percentage of total nuclei (excluding pyknotic apoptotic nuclei) in the VZ (E11.5) or VZ plus SVZ (E16.5) as revealed by DAPI staining, in *Brca1* control and cKO mice. Data are the mean of three embryos (the sum of three 200-μm-wide fields per embryo); error bars indicate s.e.m. (**C**) Numbers of total DAPI-stained nuclei (excluding pyknotic apoptotic nuclei) in the VZ (E11.5) or VZ plus SVZ (E16.5). Data are from the quantification in B; error bars indicate s.e.m.

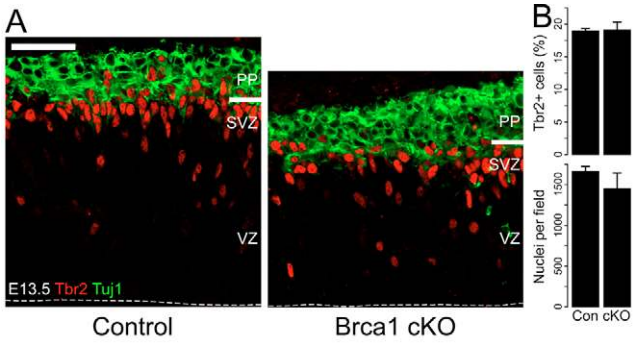


**Fig. 7. Conditional *Brca1* ablation in the dorsal telencephalon does not alter the proportion of Tbr2-positive cells.** (**A**) Double immunofluorescence (1-μm optical section) for Tbr2 (red) and Tuj1 (green) on coronal cryosections of E13.5 dorsal telencephalon of *Brca1* control (left) and cKO (right) mice. PP, preplate. Dashed lines indicate the ventricular surface. Scale bar: 50 μm. (**B**) Quantification of Tbr2$^+$ nuclei in the cortical wall, expressed as a percentage of total nuclei (excluding pyknotic apoptotic nuclei) as revealed by DAPI staining (top), and numbers of DAPI-stained total nuclei per field (bottom). Data are the mean of three embryos (the sum of three 200-μm-wide fields per embryo); error bars indicate s.e.m.

analyzed the basal (or intermediate) progenitor lineage, which is one of the major lineages of neocortical progenitors (Haubensak et al., 2004; Miyata et al., 2004; Noctor et al., 2004). Basal progenitors are delaminated non-epithelial progenitors that (1) are downstream to apical progenitors (neuroepithelial cells, radial glial cells), (2) are thought to generate the majority of neocortical neurons, and (3) are characterized by the expression of Tbr2 (Eomes) (Haubensak et al., 2004; Englund et al., 2005; Attardo et al., 2008). We performed immunofluorescence for Tbr2 on control and *Brca1*-ablated E13.5 dorsal telencephalon (Fig. 7A) and quantified the percentage of Tbr2$^+$ nuclei over total nuclei as revealed by DAPI staining (Fig. 7B, top). No significant change was found in the percentage of Tbr2$^+$ cells in the cortical wall, indicating that the *Brca1* ablation that occurred in neuroepithelial cells did not affect the subsequent generation of Tbr2$^+$ basal progenitors from apical progenitors. As shown in Fig. 3D, the number of nuclei per field in the *Brca1*-ablated E13.5 dorsal telencephalon was reduced, which mostly reflected the decrease in the radial thickness of the progenitor layers (Fig. 7B, bottom).

### *Brca1* ablation in VZ progenitors of the dorsal telencephalon results in nuclear translocation of p53

Increased apoptosis caused by *Brca1* removal is known to involve the p53 (Trp53) pathway (Lakin and Jackson, 1999; Xu et al., 2001; Fridman and Lowe, 2003). We therefore performed immunofluorescence for p53 in the E11.5 control and *Brca1*-ablated dorsal telencephalon. In the control VZ, p53 immunoreactivity was low and, when detectable, was concentrated in the perinuclear cytoplasm (Fig. 8A,B). By contrast, *Brca1*-ablated VZ progenitors (identified by PCNA immunostaining) often showed nuclear p53 immunoreactivity (Fig. 8C,D). Thus, *Brca1* ablation in the dorsal telencephalon results in the nuclear translocation of p53 and hence in the activation of the p53 pathway (Haupt et al., 1997; Fuchs et al., 1998).

## DISCUSSION

Our study shows that Brca1, the gene of which shows evidence of positive selection during primate evolution (Huttley et al., 2000), has a role in controlling the size of the cerebral cortex during mouse embryonic development by preventing the apoptosis of early cortical progenitors and their immediate progeny. The reduction in size of the *Brca1*-ablated neocortex is remarkable in that it appears to be proportional, affecting both radial thickness and lateral extension, and in that cortical layering, despite this reduction, remains largely intact. The nature of this size reduction is consistent with the apoptosis that occurs in early, but not late, progenitors and their immediate progeny, and is in accordance with the radial unit hypothesis (Rakic, 1988; Rakic, 1995), which predicts that a depletion of early progenitors results in a decrease in the lateral expansion of the neocortex. The observation that the upper-most cortical layers are not reduced upon *Brca1* ablation is consistent with the low levels of apoptosis we found in late progenitors and the neurons derived therefrom.

The apoptosis observed at early developmental stages upon *Brca1* ablation occurred not only in neurons, as indicated by the abundant TUNEL staining in the E11.5-13.5 preplate, but also in apical progenitors, as directly shown by the appearance of TUNEL staining in BrdU pulse-labeled VZ progenitors, and presumably also in basal progenitors as suggested by the substantial TUNEL staining in the SVZ. Taken together, the high levels of apoptosis observed in BrdU pulse-labeled S- and G2-phase cells, and the specific expression of *Brca1* in late G1, S and G2 phase (Gudas et al., 1996; Vaughn et al., 1996), raise the possibility that the main function of Brca1 in preventing apoptosis of neural progenitors is in the S or G2 phase. We did not observe any effect on the mitotic index of apical and

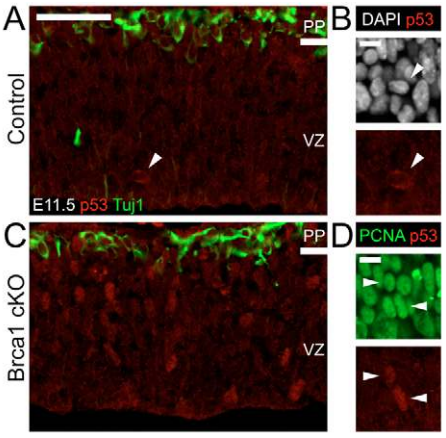


**Fig. 8. *Brca1* ablation in VZ progenitors of the dorsal telencephalon results in nuclear translocation of p53.**
(**A**,**C**) Double immunofluorescence (2-μm optical sections) for p53 (red) and Tuj1 (green) on coronal cryosections of E11.5 dorsal telencephalon of *Brca1* control (A) and cKO (C) mice. (**B**) Higher-magnification image of the cell indicated by the arrowhead in A. White, DAPI staining; red, p53 immunofluorescence. (**D**) Double immunofluorescence (2-μm optical section) for PCNA (green) and p53 (red) on a coronal cryosection of E11.5 dorsal telencephalon of a *Brca1* cKO mouse. Arrowheads indicate VZ progenitor nuclei showing p53 immunoreactivity. Scale bars: 50 μm in A,C; 10 μm in B,D.

basal progenitors or on the Tbr2 lineage, indicating that *Brca1* ablation did not affect cell cycle progression as such. Importantly, not only the nature of the reduction in size of the postnatal neocortex upon *Brca1* ablation, but also its magnitude, were fully consistent with the number of apoptotic nuclei observed for both embryonic neural progenitors and neurons.

The question arises as to what underlies the high levels of apoptosis in early but not late progenitors upon *Brca1* ablation. One possibility is that *Brca1* ablation acutely causes apoptosis in the immediate downstream progenitors and neurons, and later there is an adaptation or compensation mechanism that renders progenitors and the neurons derived therefrom less susceptible to apoptosis. Another, perhaps more intriguing possibility is that there is a difference in the properties of the early versus late cortical progenitors in either their sensitivity to *Brca1* ablation or in an intrinsic readiness to undergo apoptosis. At early stages of cortical development (up to E13.5), most apical progenitor cells divide symmetrically to proliferate (Haubensak et al., 2004), and it might be that this expanding progenitor population is more sensitive to *Brca1* ablation than the more committed, differentiating progenitors that are prevalent at later stages.

Another major difference between early and late apical progenitors is the transition from neuroepithelial to radial glial cells (Kriegstein and Götz, 2003; Götz and Huttner, 2005), and one may hypothesize that the latter are less sensitive to *Brca1* ablation. However, we find this unlikely as high levels of progenitor apoptosis were observed at E13.5, when a large proportion of apical progenitors are radial glial cells (Götz and Huttner, 2005).

A further question that arises is the molecular cause of the increased apoptosis observed upon *Brca1* ablation. In light of the observation that many VZ progenitors in the *Brca1*-ablated E11.5 dorsal telencephalon exhibited nuclear localization of p53, there are two major possibilities. First, reflecting the function of Brca1 in DNA damage repair (Scully et al., 1997a; Venkitaraman, 2001; Deng and Wang, 2003), and given that *Brca1* removal causes increased genetic instability (Shen et al., 1998; Xu et al., 1999b), there might be an increase in cells in the dorsal telencephalon that are accumulating DNA damage and undergoing apoptosis by the p53 pathway. Second, there is evidence for p53 function in mouse embryonic development, as p53-deficient mice may exhibit defects in neural tube closure (Armstrong et al., 1995; Sah et al., 1995). Increased apoptosis caused by constitutively active Notch signaling also results in nuclear localization of p53, and this increase in apoptosis is diminished in a *p53*-null background (Yang et al., 2004). Interestingly, *BRCA1* has been reported to play a significant role in the differentiation of mammary stem and progenitor cells (Liu et al., 2008). These lines of evidence raise the possibility that Brca1 might have a specific role in the development of the cerebral cortex, distinct from its function in DNA damage repair.

Alterations in the extent of apoptosis of cortical progenitors during embryonic development have been shown to greatly affect cortical size (Kuida et al., 1996; Kuida et al., 1998; Yang et al., 2004; Depaepe et al., 2005), and it has been hypothesized that regulation of neural progenitor apoptosis, especially at early developmental stages, might have contributed to the changes in neocortex size that occurred during mammalian evolution (Haydar et al., 1999; Rakic, 2005). The present study adds Brca1 to the list of key molecules required for the cerebral cortex to develop to normal size by preventing early progenitor apoptosis. Importantly, the fact that not all early progenitor cells underwent apoptosis upon *Brca1* ablation, which has also been reported with regard to the increased apoptosis upon gain of EphA receptor function (Depaepe et al., 2005) and activation of Notch signaling (Yang et al., 2004), raises the possibility that there is a subpopulation of progenitors that are particularly apoptosis prone, or that there is a stochastic mechanism that renders a certain proportion of progenitors to undergo apoptosis readily. Be this as it may, our data underscore the notion that the genetic changes that underlie cortical expansion might in particular affect the early progenitor pool (Rakic, 1988; Rakic, 1995) and implicate Brca1 as an essential component to ensure the full complement of early cortical progenitors during embryonic development.

We thank Dr Chuxia Deng and the United States National Cancer Institute, Mouse Models of Human Cancers Consortium, Mouse Repository, for kindly providing the *Brca1* conditional mutant; Dr Takuji Iwasato and Prof. Shigeyoshi Itohara, RIKEN Institute, Wako, Japan, for kindly providing the *Emx1*-Cre mouse line; Prof. Corinne Lobe, Sunnybrook and Women's College Health Science Centre, Toronto, Canada, for kindly providing the Z/EG mouse line; Jussi Helppi of the animal facility and Ronald Naumann of the transgenic core facility of MPI-CBG for excellent support; and Dr Frank Buchholz, Dr Jifeng Fei and Dr Elena Taverna for helpful comments on the manuscript. J.N.P. was a member of the International Max Planck Research School for Molecular Cell Biology and Bioengineering. W.B.H. was supported by a grant from the DFG (SFB 655, A2), by the DFG-funded Center for Regenerative Therapies Dresden, and by the Fonds der Chemischen Industrie.

**Supplementary material**
Supplementary material for this article is available at
http://dev.biologists.org/cgi/content/full/136/11/1859/DC1

**References**
**Armstrong, J. F., Kaufman, M. H., Harrison, D. J. and Clarke, A. R.** (1995). High-frequency developmental abnormalities in p53-deficient mice. *Curr. Biol.* **5**, 931-936.
**Attardo, A., Calegari, F., Haubensak, W., Wilsch-Bräuninger, M. and Huttner, W. B.** (2008). Live imaging at the onset of cortical neurogenesis reveals differential appearance of the neuronal phenotype in apical versus basal progenitor progeny. *PLoS ONE* **3**, e2388.
**Berton, T. R., Matsumoto, T., Page, A., Conti, C. J., Deng, C. X., Jorcano, J. L. and Johnson, D. G.** (2003). Tumor formation in mice with conditional inactivation of Brca1 in epithelial tissues. *Oncogene* **22**, 5415-5426.

**Bond, J. and Woods, C. G.** (2006). Cytoskeletal genes regulating brain size. *Curr. Opin. Cell Biol.* **18**, 95-101.
**Bond, J., Roberts, E., Mochida, G. H., Hampshire, D. J., Scott, S., Askham, J. M., Springell, K., Mahadevan, M., Crow, Y. J., Markham, A. F. et al.** (2002). ASPM is a major determinant of cerebral cortical size. *Nat. Genet.* **32**, 316-320.
**Buchman, J. J. and Tsai, L. H.** (2007). Spindle regulation in neural precursors of flies and mammals. *Nat. Rev. Neurosci.* **8**, 89-100.
**Bulfone, A., Smiga, S. M., Shimamura, K., Peterson, A., Puelles, L. and Rubenstein, J. L.** (1995). T-brain-1: a homolog of Brachyury whose expression defines molecularly distinct domains within the cerebral cortex. *Neuron* **15**, 63-78.
**Bystron, I., Rakic, P., Molnár, Z. and Blakemore, C.** (2006). The first neurons of the human cerebral cortex. *Nat. Neurosci.* **9**, 880-886.
**Calegari, F., Haubensak, W., Haffner, C. and Huttner, W. B.** (2005). Selective lengthening of the cell cycle in the neurogenic subpopulation of neural progenitor cells during mouse brain development. *J. Neurosci.* **25**, 6533-6538.
**Caviness, V. S. and Takahashi, T.** (1995). Proliferative events in the cerebral ventricular zone. *Brain Dev.* **17**, 159-163.
**Chen, Y., Farmer, A. A., Chen, C. F., Jones, D. C., Chen, P. L. and Lee, W. H.** (1996). BRCA1 is a 220-kDa nuclear phosphoprotein that is expressed and phosphorylated in a cell cycle-dependent manner. *Cancer Res.* **56**, 3168-3172.
**Dehay, C. and Kennedy, H.** (2007). Cell-cycle control and cortical development. *Nat. Rev. Neurosci.* **8**, 438-450.
**Dehay, C., Savatier, P., Cortay, V. and Kennedy, H.** (2001). Cell-cycle kinetics of neocortical precursors are influenced by embryonic thalamic axons. *J. Neurosci.* **21**, 201-214.
**Del Río, J. A., Martínez, A., Fonseca, M., Auladell, C. and Soriano, E.** (1995). Glutamate-like immunoreactivity and fate of Cajal-Retzius cells in the murine cortex as identified with calretinin antibody. *Cereb. Cortex* **5**, 13-21.
**Deng, C. X. and Wang, R. H.** (2003). Roles of BRCA1 in DNA damage repair: a link between development and cancer. *Hum. Mol. Genet.* **12 Spec No 1**, R113-R123.
**Depaepe, V., Suarez-Gonzalez, N., Dufour, A., Passante, L., Gorski, J. A., Jones, K. R., Ledent, C. and Vanderhaeghen, P.** (2005). Ephrin signalling controls brain size by regulating apoptosis of neural progenitors. *Nature* **435**, 1244-1250.
**Englund, C., Fink, A., Lau, C., Pham, D., Daza, R. A., Bulfone, A., Kowalczyk, T. and Hevner, R. F.** (2005). Pax6, Tbr2, and Tbr1 are expressed sequentially by radial glia, intermediate progenitor cells, and postmitotic neurons in developing neocortex. *J. Neurosci.* **25**, 247-251.
**Farkas, L. M. and Huttner, W. B.** (2008). The cell biology of neural stem and progenitor cells and its significance for their proliferation versus differentiation during mammalian brain development. *Curr. Opin. Cell Biol.* **20**, 707-715.
**Ferland, R. J., Cherry, T. J., Preware, P. O., Morrisey, E. E. and Walsh, C. A.** (2003). Characterization of Foxp2 and Foxp1 mRNA and protein in the developing and mature brain. *J. Comp. Neurol.* **460**, 266-279.
**Fish, J. L., Dehay, C., Kennedy, H. and Huttner, W. B.** (2008). Making bigger brains-the evolution of neural-progenitor-cell division. *J. Cell Sci.* **121**, 2783-2793.
**Fonseca, M., dél Río, J. A., Martínez, A., Gómez, S. and Soriano, E.** (1995). Development of calretinin immunoreactivity in the neocortex of the rat. *J. Comp. Neurol.* **361**, 177-192.
**Fridman, J. S. and Lowe, S. W.** (2003). Control of apoptosis by p53. *Oncogene* **22**, 9030-9040.
**Fuchs, S. Y., Adler, V., Buschmann, T., Wu, X. and Ronai, Z.** (1998). Mdm2 association with p53 targets its ubiquitination. *Oncogene* **17**, 2543-2547.
**Götz, M. and Huttner, W. B.** (2005). The cell biology of neurogenesis. *Nat. Rev. Mol. Cell Biol.* **6**, 777-788.
**Götz, M., Stoykova, A. and Gruss, P.** (1998). Pax6 controls radial glia differentiation in the cerebral cortex. *Neuron* **21**, 1031-1044.
**Gowen, L. C., Johnson, B. L., Latour, A. M., Sulik, K. K. and Koller, B. H.** (1996). Brca1 deficiency results in early embryonic lethality characterized by neuroepithelial abnormalities. *Nat. Genet.* **12**, 191-194.
**Gudas, J. M., Li, T., Nguyen, H., Jensen, D., Rauscher, F. J. and Cowan, K. H.** (1996). Cell cycle regulation of BRCA1 messenger RNA in human breast epithelial cells. *Cell Growth Differ.* **7**, 717-723.
**Haubensak, W., Attardo, A., Denk, W. and Huttner, W. B.** (2004). Neurons arise in the basal neuroepithelium of the early mammalian telencephalon: a major site of neurogenesis. *Proc. Natl. Acad. Sci. USA* **101**, 3196-3201.
**Haupt, Y., Maya, R., Kazaz, A. and Oren, M.** (1997). Mdm2 promotes the rapid degradation of p53. *Nature* **387**, 296-299.
**Haydar, T. F., Kuan, C. Y., Flavell, R. A. and Rakic, P.** (1999). The role of cell death in regulating the size and shape of the mammalian forebrain. *Cereb. Cortex* **9**, 621-626.
**He, X., Treacy, M. N., Simmons, D. M., Ingraham, H. A., Swanson, L. W. and Rosenfeld, M. G.** (1989). Expression of a large family of POU-domain regulatory genes in mammalian brain development. *Nature* **340**, 35-41.
**Hevner, R. F., Shi, L., Justice, N., Hsueh, Y., Sheng, M., Smiga, S., Bulfone, A., Goffinet, A. M., Campagnoni, A. T. and Rubenstein, J. L.** (2001). Tbr1 regulates differentiation of the preplate and layer 6. *Neuron* **29**, 353-366.
**Hsu, L. C. and White, R. L.** (1998). BRCA1 is associated with the centrosome during mitosis. *Proc. Natl. Acad. Sci. USA* **95**, 12983-12988.
**Huttley, G. A., Easteal, S., Southey, M. C., Tesoriero, A., Giles, G. G., McCredie, M. R., Hopper, J. L. and Venter, D. J.** (2000). Adaptive evolution of the tumour suppressor BRCA1 in humans and chimpanzees. Australian Breast Cancer Family Study. *Nat. Genet.* **25**, 410-413.
**Iwasato, T., Datwani, A., Wolf, A. M., Nishiyama, H., Taguchi, Y., Tonegawa, S., Knöpfel, T., Erzurumlu, R. S. and Itohara, S.** (2000). Cortex-restricted disruption of NMDAR1 impairs neuronal patterns in the barrel cortex. *Nature* **406**, 726-731.
**Joukov, V., Groen, A. C., Prokhorova, T., Gerson, R., White, E., Rodriguez, A., Walter, J. C. and Livingston, D. M.** (2006). The BRCA1/BARD1 heterodimer modulates ran-dependent mitotic spindle assembly. *Cell* **127**, 539-552.
**Korhonen, L., Brännvall, K., Skoglösa, Y. and Lindholm, D.** (2003). Tumor suppressor gene BRCA-1 is expressed by embryonic and adult neural stem cells and involved in cell proliferation. *J. Neurosci. Res.* **71**, 769-776.
**Kriegstein, A. R. and Götz, M.** (2003). Radial glia diversity: a matter of cell fate. *Glia* **43**, 37-43.
**Kriegstein, A. R. and Noctor, S. C.** (2004). Patterns of neuronal migration in the embryonic cortex. *Trends Neurosci.* **27**, 392-399.
**Kriegstein, A., Noctor, S. and Martínez-Cerdeño, V.** (2006). Patterns of neural stem and progenitor cell division may underlie evolutionary cortical expansion. *Nat. Rev. Neurosci.* **7**, 883-890.
**Kuida, K., Zheng, T. S., Na, S., Kuan, C., Yang, D., Karasuyama, H., Rakic, P. and Flavell, R. A.** (1996). Decreased apoptosis in the brain and premature lethality in CPP32-deficient mice. *Nature* **384**, 368-372.
**Kuida, K., Haydar, T. F., Kuan, C. Y., Gu, Y., Taya, C., Karasuyama, H., Su, M. S., Rakic, P. and Flavell, R. A.** (1998). Reduced apoptosis and cytochrome c-mediated caspase activation in mice lacking caspase 9. *Cell* **94**, 325-337.
**Lakin, N. D. and Jackson, S. P.** (1999). Regulation of p53 in response to DNA damage. *Oncogene* **18**, 7644-7655.
**Letinic, K., Zoncu, R. and Rakic, P.** (2002). Origin of GABAergic neurons in the human neocortex. *Nature* **417**, 645-649.
**Lin, S. Y., Rai, R., Li, K., Xu, Z. X. and Elledge, S. J.** (2005). BRIT1/MCPH1 is a DNA damage responsive protein that regulates the Brca1-Chk1 pathway, implicating checkpoint dysfunction in microcephaly. *Proc. Natl. Acad. Sci. USA* **102**, 15105-15109.
**Liu, S., Ginestier, C., Charafe-Jauffret, E., Foco, H., Kleer, C. G., Merajver, S. D., Dontu, G. and Wicha, M. S.** (2008). BRCA1 regulates human mammary stem/progenitor cell fate. *Proc. Natl. Acad. Sci. USA* **105**, 1680-1685.
**McEvilly, R. J., de Diaz, M. O., Schonemann, M. D., Hooshmand, F. and Rosenfeld, M. G.** (2002). Transcriptional regulation of cortical neuron migration by POU domain factors. *Science* **295**, 1528-1532.
**Miki, Y., Swensen, J., Shattuck-Eidens, D., Futreal, P. A., Harshman, K., Tavtigian, S., Liu, Q., Cochran, C., Bennett, L. M. and Ding, W.** (1994). A strong candidate for the breast and ovarian cancer susceptibility gene BRCA1. *Science* **266**, 66-71.
**Miyata, T., Kawaguchi, A., Saito, K., Kawano, M., Muto, T. and Ogawa, M.** (2004). Asymmetric production of surface-dividing and non-surface-dividing cortical progenitor cells. *Development* **131**, 3133-3145.
**Noctor, S. C., Martínez-Cerdeño, V., Ivic, L. and Kriegstein, A. R.** (2004). Cortical neurons arise in symmetric and asymmetric division zones and migrate through specific phases. *Nat. Neurosci.* **7**, 136-144.
**Northcutt, R. G. and Kaas, J. H.** (1995). The emergence and evolution of mammalian neocortex. *Trends Neurosci.* **18**, 373-379.
**Novak, A., Guo, C., Yang, W., Nagy, A. and Lobe, C. G.** (2000). Z/EG, a double reporter mouse line that expresses enhanced green fluorescent protein upon Cre-mediated excision. *Genesis* **28**, 147-155.
**Rakic, P.** (1988). Specification of cerebral cortical areas. *Science* **241**, 170-176.
**Rakic, P.** (1995). A small step for the cell, a giant leap for mankind: a hypothesis of neocortical expansion during evolution. *Trends Neurosci.* **18**, 383-388.
**Rakic, P.** (2005). Less is more: progenitor death and cortical size. *Nat. Neurosci.* **8**, 981-982.
**Rogers, J. H.** (1992). Immunohistochemical markers in rat cortex: co-localization of calretinin and calbindin-D28k with neuropeptides and GABA. *Brain Res.* **587**, 147-157.
**Ruffner, H. and Verma, I. M.** (1997). BRCA1 is a cell cycle-regulated nuclear phosphoprotein. *Proc. Natl. Acad. Sci. USA* **94**, 7138-7143.
**Sah, V. P., Attardi, L. D., Mulligan, G. J., Williams, B. O., Bronson, R. T. and Jacks, T.** (1995). A subset of p53-deficient embryos exhibit exencephaly. *Nat. Genet.* **10**, 175-180.
**Schierle, G. S., Gander, J. C., D'Orlando, C., Ceilo, M. R. and Vogt Weisenhorn, D. M.** (1997). Calretinin-immunoreactivity during postnatal development of the rat isocortex: a qualitative and quantitative study. *Cereb. Cortex* **7**, 130-142.
**Scully, R., Chen, J., Ochs, R. L., Keegan, K., Hoekstra, M., Feunteun, J. and Livingston, D. M.** (1997a). Dynamic changes of BRCA1 subnuclear location and phosphorylation state are initiated by DNA damage. *Cell* **90**, 425-435.

**Scully, R., Anderson, S. F., Chao, D. M., Wei, W., Ye, L., Young, R. A., Livingston, D. M. and Parvin, J. D.** (1997b). BRCA1 is a component of the RNA polymerase II holoenzyme. *Proc. Natl. Acad. Sci. USA* **94**, 5605-5610.
**Shen, S. X., Weaver, Z., Xu, X., Li, C., Weinstein, M., Chen, L., Guan, X. Y., Ried, T. and Deng, C. X.** (1998). A targeted disruption of the murine Brca1 gene causes gamma-irradiation hypersensitivity and genetic instability. *Oncogene* **17**, 3115-3124.
**Smart, I. H., Dehay, C., Giroud, P., Berland, M. and Kennedy, H.** (2002). Unique morphological features of the proliferative zones and postmitotic compartments of the neural epithelium giving rise to striate and extrastriate cortex in the monkey. *Cereb. Cortex* **12**, 37-53.
**Starita, L. M., Machida, Y., Sankaran, S., Elias, J. E., Griffin, K., Schlegel, B. P., Gygi, S. P. and Parvin, J. D.** (2004). BRCA1-dependent ubiquitination of gamma-tubulin regulates centrosome number. *Mol. Cell. Biol.* **24**, 8457-8466.
**Starita, L. M., Horwitz, A. A., Keogh, M. C., Ishioka, C., Parvin, J. D. and Chiba, N.** (2005). BRCA1/BARD1 ubiquitinate phosphorylated RNA polymerase II. *J. Biol. Chem.* **280**, 24498-24505.
**Takahashi, T., Nowakowski, R. S. and Caviness, V. S.** (1995). The cell cycle of the pseudostratified ventricular epithelium of the embryonic murine cerebral wall. *J. Neurosci.* **15**, 6046-6057.
**Taylor, R. C., Cullen, S. P. and Martin, S. J.** (2008). Apoptosis: controlled demolition at the cellular level. *Nat. Rev. Mol. Cell Biol.* **9**, 231-241.
**Thomaidou, D., Mione, M. C., Cavanagh, J. F. and Parnavelas, J. G.** (1997). Apoptosis and its relation to the cell cycle in the developing cerebral cortex. *J. Neurosci.* **17**, 1075-1085.
**Turner, N., Tutt, A. and Ashworth, A.** (2004). Hallmarks of 'BRCAness' in sporadic cancers. *Nat. Rev. Cancer* **4**, 814-819.
**Vaughn, J. P., Davis, P. L., Jarboe, M. D., Huper, G., Evans, A. C., Wiseman, R. W., Berchuck, A., Iglehart, J. D., Futreal, P. A. and Marks, J. R.** (1996). BRCA1 expression is induced before DNA synthesis in both normal and tumor-derived breast cells. *Cell Growth Differ.* **7**, 711-715.
**Venkitaraman, A. R.** (2001). Functions of BRCA1 and BRCA2 in the biological response to DNA damage. *J. Cell Sci.* **114**, 3591-3598.
**Wang, R. H., Yu, H. and Deng, C. X.** (2004). A requirement for breast-cancer-associated gene 1 (BRCA1) in the spindle checkpoint. *Proc. Natl. Acad. Sci. USA* **101**, 17108-17113.
**Windrem, M. S. and Finlay, B. L.** (1991). Thalamic ablations and neocortical development: alterations of cortical cytoarchitecture and cell number. *Cereb. Cortex* **1**, 230-240.
**Wonders, C. P. and Anderson, S. A.** (2006). The origin and specification of cortical interneurons. *Nat. Rev. Neurosci.* **7**, 687-696.
**Xu, X., Wagner, K. U., Larson, D., Weaver, Z., Li, C., Ried, T., Hennighausen, L., Wynshaw-Boris, A. and Deng, C. X.** (1999a). Conditional mutation of Brca1 in mammary epithelial cells results in blunted ductal morphogenesis and tumour formation. *Nat. Genet.* **22**, 37-43.
**Xu, X., Weaver, Z., Linke, S. P., Li, C., Gotay, J., Wang, X. W., Harris, C. C., Ried, T. and Deng, C. X.** (1999b). Centrosome amplification and a defective G2-M cell cycle checkpoint induce genetic instability in BRCA1 exon 11 isoform-deficient cells. *Mol. Cell* **3**, 389-395.
**Xu, X., Qiao, W., Linke, S. P., Cao, L., Li, W. M., Furth, P. A., Harris, C. C. and Deng, C. X.** (2001). Genetic interactions between tumor suppressors Brca1 and p53 in apoptosis, cell cycle and tumorigenesis. *Nat. Genet.* **28**, 266-271.
**Xu, X., Lee, J. and Stern, D. F.** (2004). Microcephalin is a DNA damage response protein involved in regulation of CHK1 and BRCA1. *J. Biol. Chem.* **279**, 34091-34094.
**Yang, X., Klein, R., Tian, X., Cheng, H. T., Kopan, R. and Shen, J.** (2004). Notch activation induces apoptosis in neural progenitor cells through a p53-dependent pathway. *Dev. Biol.* **269**, 81-94.
**Zhong, X., Liu, L., Zhao, A., Pfeifer, G. P. and Xu, X.** (2005). The abnormal spindle-like, microcephaly-associated (ASPM) gene encodes a centrosomal protein. *Cell Cycle* **4**, 1227-1229.